# Superstatistical two-temperature Ising model

J. Cheraghalizadeh,* M. Seifi,† Z. Ebadi,‡ H. Mohammadzadeh,§ and M. N. Najafi‖
*Department of Physics, University of Mohaghegh Ardabili, P.O. Box 179, Ardabil, Iran*

(Received 1 August 2020; revised 5 January 2021; accepted 12 February 2021; published 4 March 2021)

The previous approach of the nonequilibrium Ising model was based on the local temperature in which each site or part of the system has its own specific temperature. We introduce an approach of the two-temperature Ising model as a prototype of the superstatistic critical phenomena. The model is described by two temperatures $(T_1, T_2)$ in a zero magnetic field. To predict the phase diagram and numerically estimate the exponents, we develop the Metropolis and Swendsen-Wang Monte Carlo method. We observe that there is a nontrivial critical line, separating ordered and disordered phases. We propose an analytic equation for the critical line in the phase diagram. Our numerical estimation of the critical exponents illustrates that all points on the critical line belong to the ordinary Ising universality class.

DOI: 10.1103/PhysRevE.103.032104

## I. INTRODUCTION

"What is the impact of the fluctuations in macroscopic parameters, such as the temperature?" is a long-standing question in the thermodynamics and statistical mechanics, and generally in physics. Although the fluctuations in temperature bring the system to the *out-of-equilibrium phenomena* category, some key concepts of equilibrium thermodynamics can be employed in studying them. Superstatistics is an example of a systematic way of handling such fluctuations, which cannot be defined uniquely in general terms. It generally is called *the statistics of the statistics*, which itself can be translated to a modified Boltzmann factor [that is $\exp(-\beta E)$ in the equilibrium systems, where $\beta$ and $E$ are the usual inverse temperature and the energy, respectively], whose parameters have relations with the fluctuations of the thermodynamic quantities, such as the temperature [1]. In this view, superstatistics is served as a systematic way that uses superpositions of various Boltzmann distributions [1], which was propounded by Beck and Cohen [1] and Beck [2] with a primitive goal of modeling the non-Maxwell-Boltzmann statistical distributions in out-of-equilibrium complex systems. The fact that makes these systems tractable is that the fluctuations in macroscopic parameters are mostly in long timescales so that the system can temporarily reach local equilibrium [3]. This leads to a common approach where one adjusts the conditional probabilities of the fluctuating system with the probability measures in the systems without fluctuations. The superstatistics has been employed in many physical systems, such as nuclear physics [4], turbulent fluids [3,5–7], solar flares [8], ultracold gases [9,10], and quantum entanglement [11,12].

Actually the Tsallis statistics and the Levy distributions were earlier examples of superstatistics [4] for which it was shown that the nonextensivity is given by the fluctuations of the parameters of the usual exponential distributions. The microscopic fluctuations (in the random friction forces) also were shown to lead to effective nonextensive statistical mechanics. This might serve as the mechanism behind the fact that many physical systems with fluctuating temperature or energy dissipation rate are described by the Tsallis statistics [7].

There are many strategies to implement temperature fluctuations, such as *quenched distribution*, or the annealed one. In the first strategy, one distributes the temperature throughout the system, having local equilibrium described by the Boltzmann factor. A simple model to describe such a strategy was proposed by Garrido *et al.* [13] for the Ising model where the ferroparamagnetism phase transition was observed. The focus of it was to explain the system in terms of two (and can be extended to more) locally competing temperatures by considering the spin-flip probability of each site as $p$ if it were in contact with a thermal bath at the temperature $T - \Delta T$, and $1 - p$ if the temperature of the bath were at $T + \Delta T$; $T \geqslant \Delta T > 0$. In another study, based on the heat bath to which each site or band with a single temperature is coupled, Tamayo *et al.* [14] expanded this concept and made a comparative study of the system with a focus on the critical behaviors, showing that the transition point belongs to the same universality class as the equilibrium two-dimensional Ising model. Also they showed that the band version of the Swendsen-Wang (SW) update algorithm can be mapped into an equilibrium model at an effective temperature. Similar works have been introduced and developed based on local temperatures and focused on coupling different models with two (or more) thermal baths [15–17]. For another example, Ref. [18] using two sublattices at different temperatures, showed that the critical properties of

*jafarcheraghalizadeh@gmail.com
†maryam.seifi.physics@gmail.com
‡zahraa.ebadi@gmail.com
§h.mohammadzadeh@gmail.com
‖morteza.nattagh@gmail.com

 

these nonequilibrium systems fit well with the Ising universality class. A two-dimensional half-filled lattice gas model with nearest-neighbor attractive interaction can be found in Ref. [19] where the authors assumed that the particles are coupled to two thermal baths at different temperatures. Kawasaki dynamics for the Ising model is another instance for which the effect of two (parallel or perpendicular) temperatures were analyzed numerically [20] and analytically [21]. An antiferromagnet Ising system in two dimensions with a heat bath [22] and the analysis of the interfaces in a nonequilibrium two-temperature Ising model [22] are other studies that can be mentioned in this context.

In the second category, one manipulates the Boltzmann factor by, e.g., superposition of them. This methodology has proved to be very effective in describing various systems [1,2,4,5,8]. Despite huge literature in the application of superstatistics in nonequilibrium systems [23–25] and extensive discussions on the two-temperature Ising model based on locally competing temperatures (or heat baths) in which a site or a part of a system with different probability stays at different temperatures, very little attention has been paid to superstatistic critical phenomena in this category. More explicitly what is the effect of the superposition of Boltzmann factors with different temperatures (second category for fluctuations in the parameters) in statistical models, especially in the vicinity of the critical points? Here we use the term *superstatistic critical phenomena* (SCP) for this area. As a start we consider a two-dimensional Ising model with two temperatures $(T_1, T_2)$ with a zero magnetic field so that each site or band *fluctuates between two temperatures*. We note that this is different from the first category, i.e., the models that are reviewed above for which each region has its own temperature. Our motivation for choosing the Ising model is that it is extensively used in statistical mechanics as a prototype of an equilibrium system which undergoes nontrivial phase transition, the main one being order-disorder transition at a critical temperature $T_c$ in the absence of a magnetic field. Many interesting aspects of this model are known [26]. This involves the coexistence of percolation and magnetic phase transition [27], elastic backbone transition [28], equivalence to Schramm-Loewner evolution with $\kappa = 2$ [29], probability measure of the order parameter [30], and its relation to the free fermionic model [31,32]. Also the Ising model has vastly been used as a partner for other combined statistical models. The example is the self-organization critically on the Ising-percolation lattices (the movement pattern of fluid in the Ising-correlated porous media) [33–38]. It is also used as a host for various random walks [39,40]. In light of the known properties of the Ising model, especially in the vicinity of the critical point, we are able to recover many aspects of the SCP.

We construct a superstatistic binary Ising model (the second category) and develop Metropolis and the SW) Monte Carlo method [41] for investigating the system numerically and analytically. We show that the order-disorder phase transition takes place over an extended line. By extracting various exponents, we illustrate that the universality class of all points on the critical line is consistent with the ordinary Ising universality class.

The paper is organized as follows: In the next section we introduce the problem with binary distribution. The model is introduced in this section, along with the Metropolis and SW algorithms. The numerical results are presented in Sec. III where we explore the properties of the extended critical line. We close the paper with a conclusion.

## II. THE CONSTRUCTION OF THE PROBLEM

The stationary probability density of an equilibrium system is described by the Boltzmann factors $\exp(-\beta E)$, where $\beta$ is the inverse of temperature and $E$ is the system energy. For out-of-equilibrium systems this law is replaced by other more sophisticated scenarios, ranging from Einstein's relation of fluctuations [1] to local equilibrium systems with temperature varying from place to place. This latter case has been explored much in the literature by concentrating in most cases on the Ising model as explored in the previous section as the first category. In the second category the system is described by a superposition of Boltzmann factors. For this case the generalized Boltzmann factor is defined as follows [3]:

$$B(E) = \int_0^\infty f(\beta) e^{-\beta E} d\beta, \tag{1}$$

where $f(\beta)$ is a superstatistical kernel, and $E$ is the total energy of the system in the respective microstate. Indeed the probability distribution of $\beta$ reads

$$p(E) = \frac{1}{Z} B(E), \tag{2}$$

where

$$Z = \int_0^\infty B(E) dE. \tag{3}$$

The kernel is positive and normalized [i.e., $\int_0^\infty f(\beta) d\beta = 1$]. For a fixed nonfluctuating temperature $\frac{1}{\beta_0}$, the kernel is $f(\beta) = \delta(\beta - \beta_0)$, and, consequently, $B(E)$ is an ordinary Boltzmann factor, where $\delta$ is the Dirac $\delta$ function. Various superstatistical kernels have been investigated in Refs. [1,42,43].

The simplest generalization of Boltzmann factor is a system with two temperatures (i.e., the system which fluctuates between two different discrete values of the temperatures $\beta_1 = \frac{1}{T_1}$ and $\beta_2 = \frac{1}{T_2}$ with a same probability). The probability distribution of $\beta$ is given by

$$f(\beta) = \tfrac{1}{2}[\delta(\beta - \beta_1) + \delta(\beta - \beta_2)]. \tag{4}$$

The generalization of above distribution to $n$ temperatures is straightforward. The important question here is how the properties of the model at hand (the Ising model here) are changed under this generalization. Using Eq. (1), a generalized Boltzmann factor is obtained which we call the two-level Boltzmann factor (2LBF) as follows:

$$B(E) = \tfrac{1}{2}(e^{-\beta_1 E} + e^{-\beta_2 E}). \tag{5}$$

This is renormalizable only for $E \geqslant 0$ [1]. In the rest of the paper, we focus on the application of 2LBF on the two-dimensional Ising model on a square lattice. The classical Ising model is defined via the dynamic of spins $\sigma$ described by the Ising Hamiltonian,

$$H = -J \sum_{\langle i,j \rangle} \sigma_i \sigma_j - h \sum_i \sigma_i, \tag{6}$$

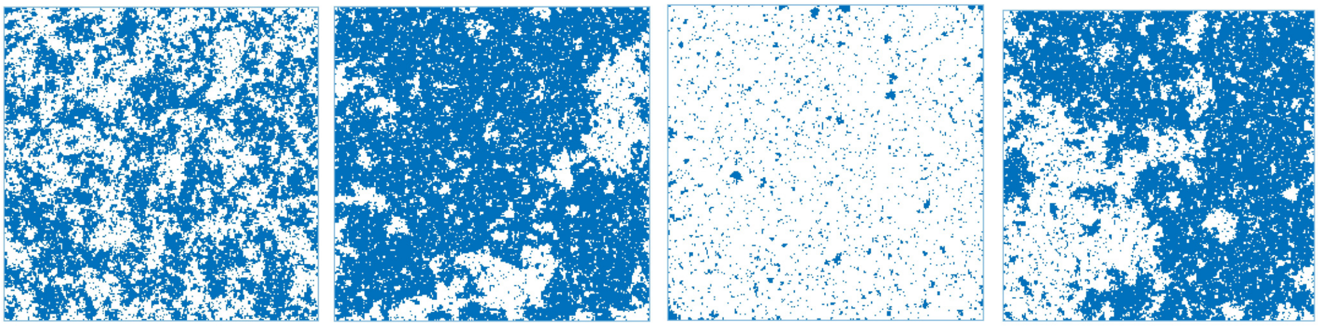

(a) $T_2 = 2.50$ , $T_1 = 0.001$. (b) $T_2 = 2.50$ , $T_1 \approx T_1^{c_1}$. (c) $T_2 = 2.50$ , $T_1 = 1.50$. (d) $T_2 = 2.50$ , $T_1 \approx T_1^{c_2}$.

FIG. 1. The Ising samples by the SW algorithm in $256 \times 256$ lattice size at fixed $T_2 = 2.50$ for four variant temperatures ($T_1$). For all fixed temperatures between regular Ising critical temperature ($T_c \approx 2.26\,918$) and $T_D^{\vDash}$ there are two critical points. The white sites show spin up, and the blue sites show spin down.

where $J$ is the coupling constant, $h$ is the magnetic field which is set to zero in this paper, and $\langle i, j\rangle$ shows that the sites $i$ and $j$ are neighbors. The spins $\sigma_i$ at each site $i$ take two values $\pm 1$. We would use free boundary conditions for all cases in the paper.

For investigating the Ising model with 2LBF, we first should develop Metropolis Monte Carlo schemes for the numerical procedures. A good starting point is to follow the same strategy as the one-temperature Ising model for which under a single spin flip the total energy is changed to $E' = E + \delta E$, where $\delta E$ is the energy excess gained by the flip. According to the Metropolis method for a single-temperature system, the probability of accepting this operation is $p = \min[1, p^{\text{single temperature}}(\beta_0)]$ in which

$$p^{\text{single temperature}}(\beta_0) = \frac{e^{-\beta_0 E'}}{e^{-\beta_0 E}} = e^{-\beta_0 \delta E}. \tag{7}$$

To generalize this for the two-temperature Ising model using the generalized Boltzmann factor in Eq. (5), we follow the same line of thinking, this time for 2LBFs. To this end, we use the ratio of the probabilities, which is valid only for $E \geqslant 0$,

$$\begin{aligned} p^{\text{2LBF}}(\beta_1, \beta_2) &\equiv \frac{B(E')}{B(E)} \\ &= \frac{e^{-\beta_1 \delta E}}{1 + e^{(\beta_1 - \beta_2)E}} + \frac{e^{-\beta_2 \delta E}}{1 + e^{-(\beta_1 - \beta_2)E}}, \end{aligned} \tag{8}$$

which readily reduces to $p^{\text{single temperature}}(\beta_0)$ in the limit $\beta_1 = \beta_2 = \beta_0$. For $E < 0$, however, this relation is not valid since $B_E$ is not normalizable [1] for which $p^{\text{2LBF}}(\beta_1, \beta_2)$ becomes inconsistent ( note that in $\beta_2 \to \infty$ it becomes $e^{-\beta_2 \delta E}$, which is inconsistent with our expectation from the single-temperature Ising model). This is not a problem for the system with single temperature since the extra factor in the denominator is not present, and $p$ depends only on $\delta E$. We resolve this problem by generalizing this equation to the following form:

$$p^{\text{2LBF}}(\beta_1, \beta_2) = \frac{e^{-\beta_1 \delta E}}{1 + e^{(\beta_1 - \beta_2)|E|}} + \frac{e^{-\beta_2 \delta E}}{1 + e^{-(\beta_1 - \beta_2)|E|}}, \tag{9}$$

where $|E|$ is the absolute value of $E$. One can easily check that the ordinary Metropolis results are obtained for $\beta_1 \to \infty$, $\beta_2 \to \infty$, or $\beta_1 = \beta_2$, no matter if $E$ is positive or negative. We also show in the following that this generalization gives consistent results. For simulations, system starts from a random spin configuration and in each step choose a site randomly and apply the flip with probability:

$$p = \min[1, p^{\text{2LBF}}(\beta_1, \beta_2)]. \tag{10}$$

For each coupled temperature ($T_1, T_2$), this process continues until reaching a stationary state in the energy landscape. Some example has been shown in Fig. 2.

The other method that we use is the Swendsen-Wang algorithm [41] in which instead of a single spin flip, a cluster, namely, the Fortuin-Kasteleyn (FK) cluster [44] is chosen to flip [41]. To define FK clusters, let us define first the geometric spin cluster, which is the connected cluster formed by sites with the same spins. The FK cluster is obtained by link dilution between the neighboring sites in the geometric spin cluster. This dilution is performed in an ordinary (single-temperature) Ising system using the following probability for establishing the links between neighboring sites $P_{\text{dialation}} = 1 - P_{\text{link}}$, where

$$P_{\text{link}} = 1 - e^{-2\beta_0}. \tag{11}$$

The overall process is just like the Metropolis method. It starts from a random configuration, and the Monte Carlo steps continues until reaching the stationary state. The SW algorithm is more appropriate in the vicinity of the critical points where the fluctuations rise, and the system falls in the problem of critical slowing down. Practically, for the Metropolis method it is more appropriate to start in the high-temperature limit and reduce the temperature slowly, whereas one can generate the samples at any given temperature using the SW algorithm. Now let us consider two-temperature case with 2LBF where instead of Eq. (11), we propose the following probability of adding a spin to the cluster:

$$P^s_{\text{link}} = \frac{1 - e^{-2\beta_1}}{1 + e^{2(\beta_1 - \beta_2)}} + \frac{1 - e^{-2\beta_2}}{1 + e^{-2(\beta_1 - \beta_2)}}. \tag{12}$$

This relation is a conjecture which is consistent with Eqs. (7), (8), and (11) and gives the expected results with respect to the Metropolis method. This relation was obtained by searching between plenty of functions that match best with the results of

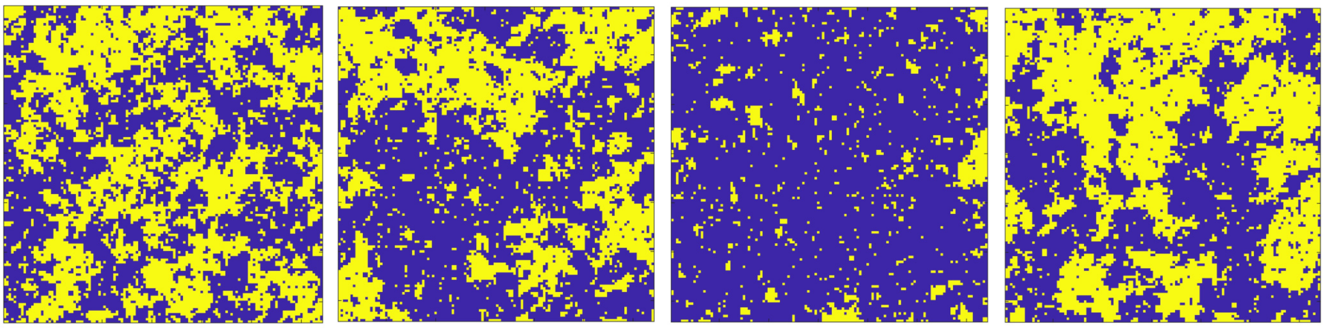

(a) $T_2 = 2.50$ , $T_1 = 0.001$. (b) $T_2 = 2.50$ , $T_1 \approx T_1^{c_1}$. (c) $T_2 = 2.50$ , $T_1 = 1.50$. (d) $T_2 = 2.50$ , $T_1 \approx T_1^{c_2}$.

FIG. 2. The Ising samples by Metropolis steps in 128 × 128 lattice size at fixed $T_2 = 2.50$ for four variant temperatures ($T_1$). For all fixed temperatures between regular Ising critical temperature ($T_c \approx 2.26\,918$) and $T_D^{\models}$ there are two critical points. The yellow sites show spin up, and the blue sites show spin down.

Metropolis. Actually, the set of functions that have the correct asymptotic behavior and match with Eqs. (7), (8), and (11) are not big. Its generalization for the $q$-state $n$-temperature Potts model is presented in Appendix. One can easily check that this probability and the probability presented in Eq. (8) are not trivially related to the one-temperature counterparts. For example, one might try to make a connection with the one-temperature system by fixing $\beta_2$ and changing $\beta_1$ leading the system to undergo an order-disorder transition. The probability measures are, however, very different from a one-temperature system in this case, meaning that one cannot define an effective temperature in the one-temperature system with a well-defined Boltzmann factor equivalent to this 2LBF system, which makes the properties of the system different and nontrivial.

In this paper we applied both algorithms for comparison reasons. Some samples that were obtained using these algorithms are shown in Fig. 1 (using the SW algorithm) and Fig. 2 (using the Metropolis algorithm).

We observed that this system undergoes order-disorder transition which defines an extended critical line. Let us define $T_c \equiv (T_1^c, T_2^c)$ as the critical points that transition takes place. In obtaining the phase diagram we fix one-temperature (say $T_2$) and change the other one ($T_1$).

Let us define the transition points by $T_{1,2}^{c_i}$ as the $i$th critical temperature for fixed $T_{2,1}$ where depending on the imposed conditions (chosen value for fixed temperature) there are zero, one ($i \in \{1\}$) or two ($i \in \{1, 2\}$) transition points.

One of the measures/observables for detecting criticality and extracting exponents is the heat capacity,

$$C_v = N(\langle E^2 \rangle - \langle E \rangle^2), \tag{13}$$

where $\langle\,\rangle$ represents ensemble average. The other quantity is the Binder cumulant also known as the fourth-order cumulant,

$$U_4 = 1 - \frac{\langle m^4 \rangle}{3\langle m^2 \rangle^2}, \tag{14}$$

where $\langle m^4 \rangle$ is the fourth moment of magnetization ($m \equiv \frac{1}{N}\sum_{i=1}^N s_i$ for each sample, and $N = L^2$ is the number of sites in the sample ) and $\langle m^2 \rangle$ is second moment of the magnetization. It has been defined as the kurtosis of the order parameter. The phase-transition point is usually identified comparing the behavior of $U_4$ as a function of the temperature for different values of the system size $L$.

Also, the magnetic susceptibility which is defined by

$$\chi = N(\langle m^2 \rangle - \langle m \rangle^2) \tag{15}$$

is calculated in this paper which is expected to diverge in a power-law fashion at the continuous phase transition.

## III. NUMERICAL RESULTS

We used $L = 64$, 128, 256, 512, and 1024 and $L = 128$, 256, and 512 lattice sizes for SW and Metropolis algorithms, respectively. We fixed $T_2$ and ran the program (for both Metropolis and SW algorithms) starting from high temperatures of $T_1$. The ensemble averages were performed upon $10^4$ samples.

Before going to details, let us summarize the main results which facilitate reading the rest of paper.

The phase diagram is shown in Fig. 3 where the bold circles are the transition points obtained by simulations, and the black bold line is the interpolation between points to help the eye.

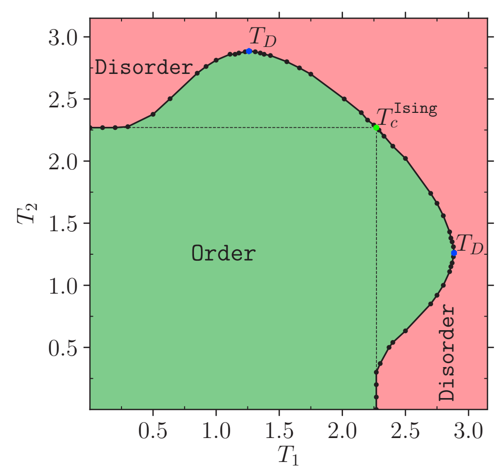


FIG. 3. The phase diagram for $T_1$ and $T_2$. The read area indicates the disorder phase, and the green area indicates the order phase.

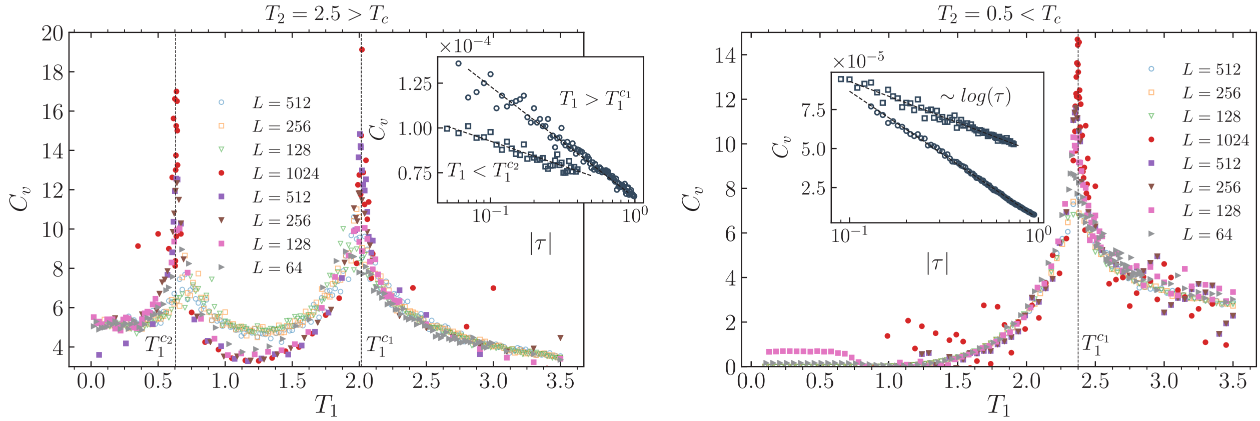


(a) (b)

FIG. 4. (a) Heat-capacity ($C_v$) for various system sizes in fixed $T_2 = 2.5 > T_c$. The inset: The critical exponent for $C_v$ is a logarithmic scale for $T_1 > T_1^{c_2}$ and $T_1 < T_1^{c_1}$ where $\alpha = 0$. (b) Heat-capacity ($C_v$) for various system sizes in fixed $T_2 = 0.50 < T_c$. The inset: The critical exponent for $C_v$ is a logarithmic scale for $T_1 > T_1^{c_1}$ and $T_1 < T_1^{c_1}$ where $\alpha = 0$. [The filled markers represent the SW algorithm, and hollow markers represent the Metropolis algorithm].

At $T_2 = 0$, the system undergoes a continuous transition at $T_1^c \approx 2.269$ as expected for the Ising model on the square lattice. Also, one can distinguish a $T_1 \leftrightarrow T_2$ symmetry in this phase diagram as expected. We see in this figure that in the $T_2$ direction there is a highest point $T_D \equiv (T_D^{\vdash}, T_D^{\models})$ (which we estimated to be $T_D^{\vdash} = 1.270 \pm 0.003$ and $T_D^{\models} = 2.885 \pm 0.003$) which separates the properties of the model. More precisely, when we fix $T_2$ for $0 < T_2 \leqslant T_c^{\text{Ising}}$ ($T_c^{\text{Ising}}$ being the critical temperature for the ordinary two-dimensional Ising model) we have one second-order transition point for $T_1$, and for $T_c^{\text{Ising}} < T_2 < T_D^{\models}$ we have two second-order transition points for $T_1$, and for $T_2 = T_D^{\models}$ these two transition points merge so that we have one critical point for $T_1$, and for $T_2 > T_D^{\models}$ there is no transition. In the remaining we characterize this transition.

The same features are seen in terms of $T_1$, i.e., if we increase $T_2$ slowly from zero, the critical point starts to increase and gets away from $T_c^{\text{Ising}}$ up to the point $T_D^{\vdash}$ after which the critical point stars to decrease until passing $T_D^{\models}$ and reaches $T_2 = T_c^{\text{Ising}}$.

The results for the heat capacity are shown in Figs. 4(a) and 4(b) at fixed $T_2 = 2.50 > T_c^{\text{Ising}}$ and $T_2 = 0.50 < T_c^{\text{Ising}}$ in terms of $T_1$ for various system sizes. As claimed above we see that two second-order phase transitions occur at $T_1^{c_1} = 2.015 \pm 0.005$ and $T_1^{c_2} = 0.630 \pm 0.005$ when $T_2 = 2.50 > T_c^{\text{Ising}}$ in Fig. 4(a), and a second-order phase transition at fixed temperature $T_2 = 0.50 < T_c$ at $T_1^{c_2} = 2.375 \pm 0.005$ in Fig. 4(b). According to the inset of Fig. 4(a), this function behaves logarithmically in terms of $\tau$ ($\tau = T_1 - T_1^{c_1}$ for $T_1 > T_1^{c_1}$ and $\tau = T_1^{c_2} - T_1$ for $T_1 < T_1^{c_2}$) so that the $\alpha$ exponent in the two cases is zero as the same as the regular Ising model. Figure 4(b) shows similarly that the $\alpha$ exponent for $T_2 = 0.50$ is zero either $T_1 > T_1^{c_1}$ or $T_1 < T_1^{c_1}$. For comparison of two different simulation methods we have shown the results for both SW and Metropolis Monte Carlo methods.

The Binder cumulant analysis is shown in Figs. 5(a) and 5(b) in terms of $T_1$ again in fixed $T_2 = 2.50$ and $T_2 = 0.50$, respectively. These figures confirm the results of heat capacity, i.e., two critical points are seen for the fixed temperature $T_2 = 2.50$ at $T_1^{c_1} = 2.020 \pm 0.005$ and $T_1^{c_2} = 0.634 \pm 0.005$, and one critical point for $T_2 = 0.50$ at $T_1^{c_2} = 2.380 \pm 0.005$. In these figures the solid lines show the SW algorithm, and symbols represent the Metropolis method. Note that the fixed-point value for the Binder cumulant in the free boundary condition is near 0.4 as mentioned in Ref. [45], although it can be changed by other boundary conditions.

The magnetic susceptibility is shown in Figs. 6(a) and 6(b) for various system sizes in fixed $T_2 = 2.50$ and $T_2 = 0.50$, respectively, where the similar results are obtained, i.e., $T_1^{c_1} = 2.015 \pm 0.005$ and $T_1^{c_2} = 0.633 \pm 0.005$ for the first case, and $T_1^{c_2} = 2.375 \pm 0.005$ for the latter case. The scaling hypothesis predicts that the maximum value of $\chi$ at the transition point behaviors, such as $\chi_{max} \sim L^{\gamma/\nu}$. The insets in Fig. 6 shows that $\gamma/\nu = 1.75 \pm 0.01$. It is equal to the Ising critical exponent in which $\gamma/\nu = 7/4$. We observed that this is the case (for all exponents that we found in this paper) for all transition points for temperatures below $T_D^{\models}$.

The scaling behavior of $\langle m\rangle$ gives us some other important exponents. By tracking the behavior of this function in terms of $T_1$ and $L$ (for fixed $T_2$), one can extract the critical temperature $T_1^{c_{1,2}}$ as performed in Fig. 7 in which for a best choose of $\beta/\nu$ all curves cross each other in a critical point, defined via the following scaling relation:

$$m(\epsilon) = L^{-\beta/\nu} G_m(\epsilon L^{1/\nu}), \tag{16}$$

where $\epsilon \equiv \frac{T_1 - T_1^{c_{1,2}}}{T_1^{c_{1,2}}}$, $G_m(x)$ is a scaling function with $G_m(x)|_{x\to\infty} \propto x^{\beta}$ and is analytic and finite as $x \to 0$. From this analysis, we observed the above results for the critical temperatures. By plotting $\langle m\rangle L^{\beta/\nu}$ in terms of $T_1$, we found that $\beta/\nu = 0.13 \pm 0.05$ and $\nu = 1.00 \pm 0.05$, just the same as the regular Ising model. This result is correct for all temperatures on the critical line.

As seen in Fig. 8(a) and its inset, in $T_D^{\models}$ whereas there is only one transition point with the same exponents as other points, e.g., $\beta/\nu = 0.13 \pm 0.02$, the system is unable to enter

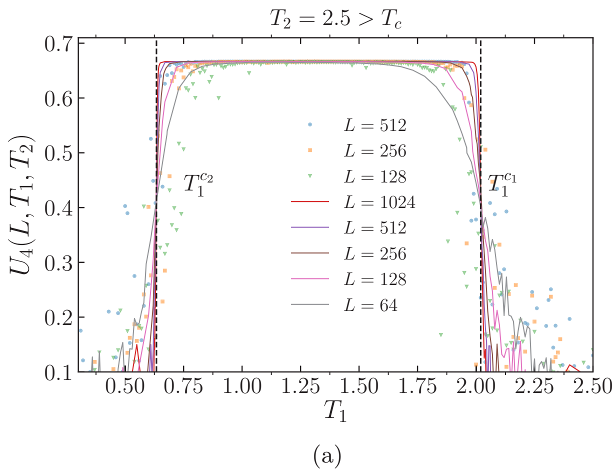


FIG. 5. (a) Binder's cumulant ($U_4$) in terms of $T_1$ for various system sizes in fixed $T_2 = 2.50 > T_c$. (b) Binder's cumulant for various system sizes in fixed $T_2 = 0.50 < T_c$. [The solid line represents the SW algorithm, and the hollow marker is the Metropolis method].

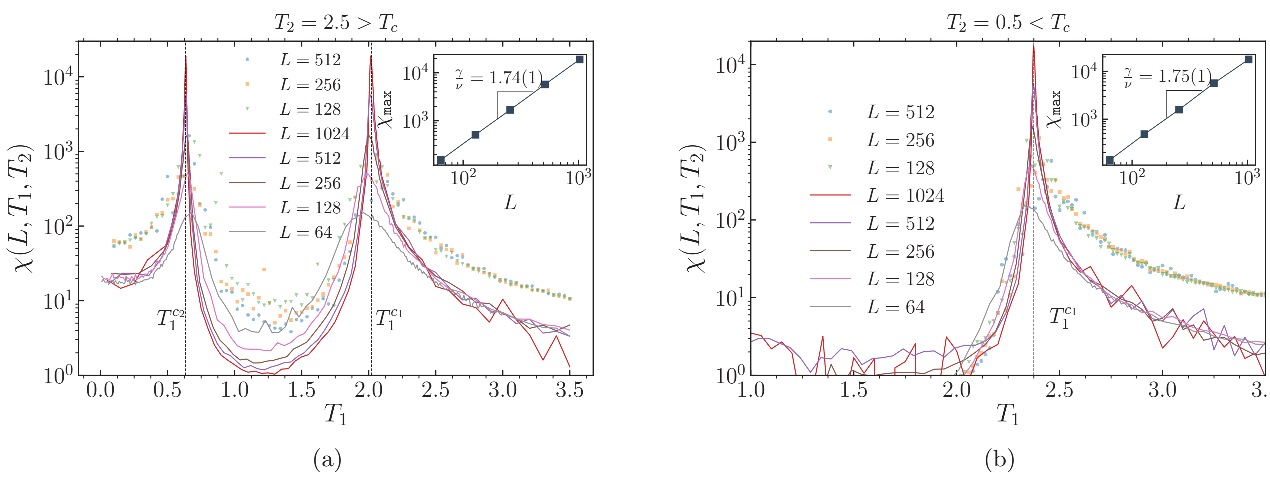


FIG. 6. (a) Magnetic susceptibility ($\chi$) for various system sizes in fixed $T_2 = 2.50 > T_c$. The inset: $\chi_{\max}$ in terms of the lattice size in which shows the $\gamma/\nu$ exponent. (b) Magnetic susceptibility in fixed $T_2 = 0.50 < T_c$. The inset: $\chi_{\max}$ in terms of the lattice size in which shows the $\gamma/\nu$ exponent. [The solid line represents the SW algorithm, and the hollow marker is the Metropolis method].

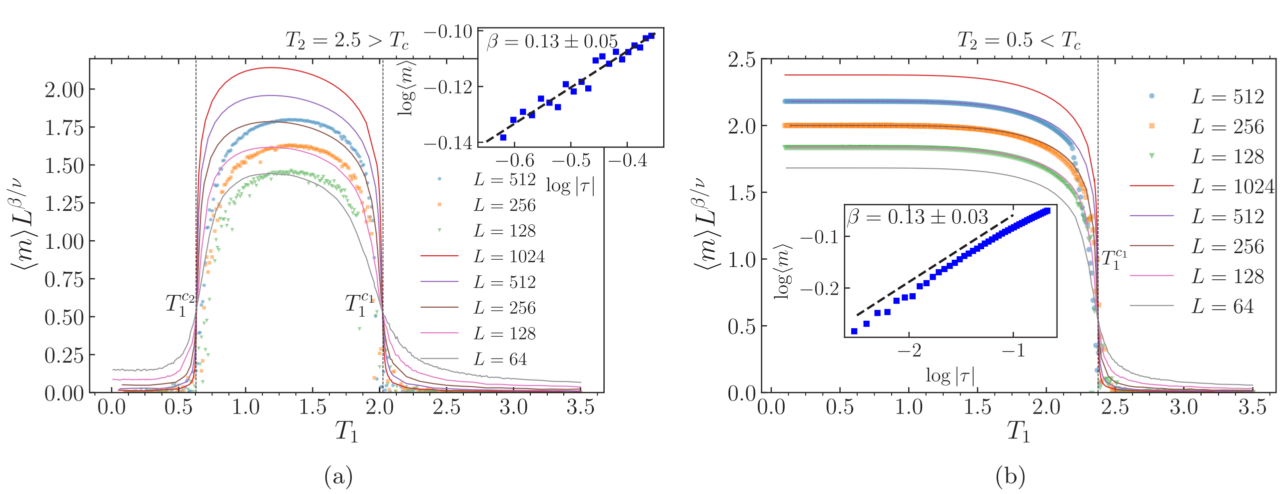


FIG. 7. (a) $\langle m \rangle L^{\beta/\nu}$ in terms of $T_1$ for various system sizes in fixed $T_2 = 2.50 > T_c$. The inset: $\langle m \rangle \sim |\tau|^{\beta}$ in which $\beta = 0.13 \pm 0.05$. (b) $\langle m \rangle L^{\beta/\nu}$ in terms of $T_1$ for various system sizes in fixed $T_2 = 0.50 < T_c$. The inset: $\langle m \rangle \sim |\tau|^{\beta}$ in which $\beta = 0.13 \pm 0.3$. [The solid line represents the SW algorithm, and the hollow marker is the Metropolis method].

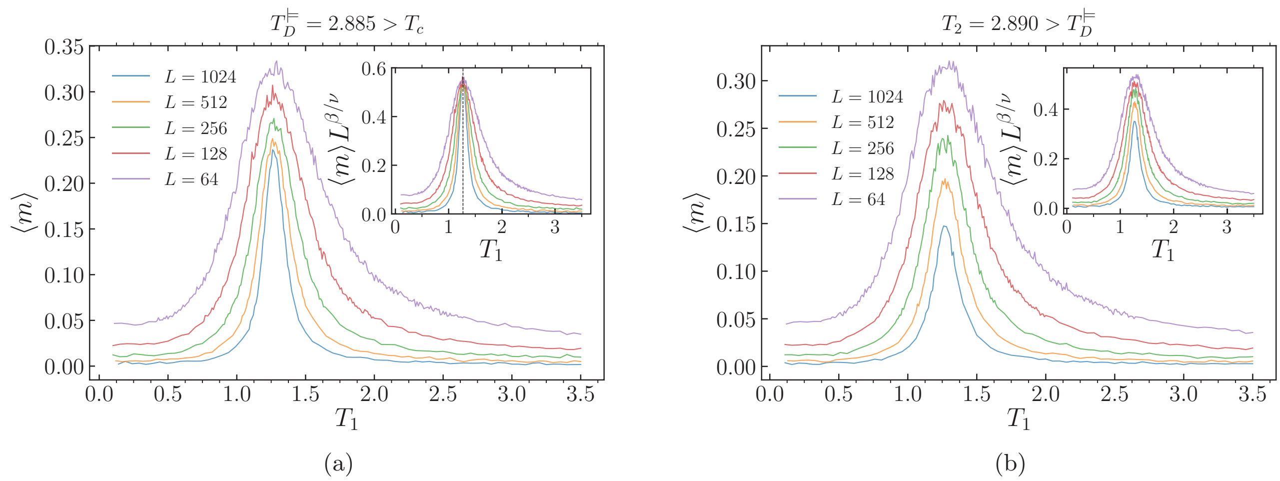


FIG. 8. (a) $\langle m \rangle$ in terms of $T_1$ for various system sizes in fixed $T_D^{\models} = 2.885 > T_c$. The inset: $\langle m \rangle L^{\beta/\nu}$ in terms of $T_1$ for various system sizes. (b) $\langle m \rangle$ in terms of $T_1$ for various system sizes in fixed $T_2 = 2.890 > T_D^{\models}$, and the inset: $\langle m \rangle \sim |\tau|^{\beta}$ in which the curves do not cross each other.

the ordered phase and, Fig. 9(a) shows that $\gamma/\nu = 1.74 \pm 0.01$ for this case. When we go a bit above this point the system is always in the disordered phase. As shown in Fig. 8(b), especially in its inset, $\beta/\nu$ does not exist that all curves cross each other in a point, and in the inset of Fig. 9(b) we observe that the exponent of $\chi_{max}$ for this case is $\mu = 1.62 \pm 0.02$. Note that it is not a critical exponent. It is only an exponent to show the difference between $T_D^{\models} = 2.885 > T_c$ and $T_2 = 2.890 > T_D^{\models}$. In fact, the maximum of the susceptibility would saturate to a constant value for large $L$ in the out of the critical region.

As the final point, let us discuss about how one can understand the form of the transition line, i.e., Fig. 3 from an analytical point of view. To this end, we compare the link probabilities of a single-temperature Ising system [i.e., Eq. (11)] with the two-temperature system [i.e., Eq. (12)]. The fact that all points in the critical line have the same properties as the Ising universality class, leads us to try finding an equivalent effective Ising system with an effective temperature $T_{\text{eff}}$, or, equivalently, $\beta_{\text{eff}} \equiv 1/T_{\text{eff}}$. Since the critical properties of the Ising model in the vicinity of the critical point is reflected in the properties of the FK clusters, which itself depends on the value of $P_{\text{link}}$, for the equivalent system we try the following equality, i.e., Eqs. (11) and (12):

$$1 - e^{-2\beta_{\text{eff}}} = \frac{1 - e^{-2\beta_1}}{1 + e^{2(\beta_1 - \beta_2)}} + \frac{1 - e^{-2\beta_2}}{1 + e^{-2(\beta_1 - \beta_2)}}. \quad (17)$$

The real solution of this equation with respect to $\beta_{\text{eff}}$ is

$$\beta_{\text{eff}}(\beta_1, \beta_2) = \frac{1}{2}\left[\ln\left(\frac{e^{2\beta_1} + e^{2\beta_2}}{e^{2(\beta_1-\beta_2)} + e^{2(\beta_2-\beta_1)}}\right)\right]. \quad (18)$$

The contour plot of this solution is shown in Fig. 10(a) in which the critical points that we found in this paper, which are blue bold circles, coincide with the contour line corresponding to $\beta_{\text{eff}}(\beta_1, \beta_2) = T_c^{\text{Ising}}$. Note that we define an effective $\beta$ only for the dilution process, keeping in mind that

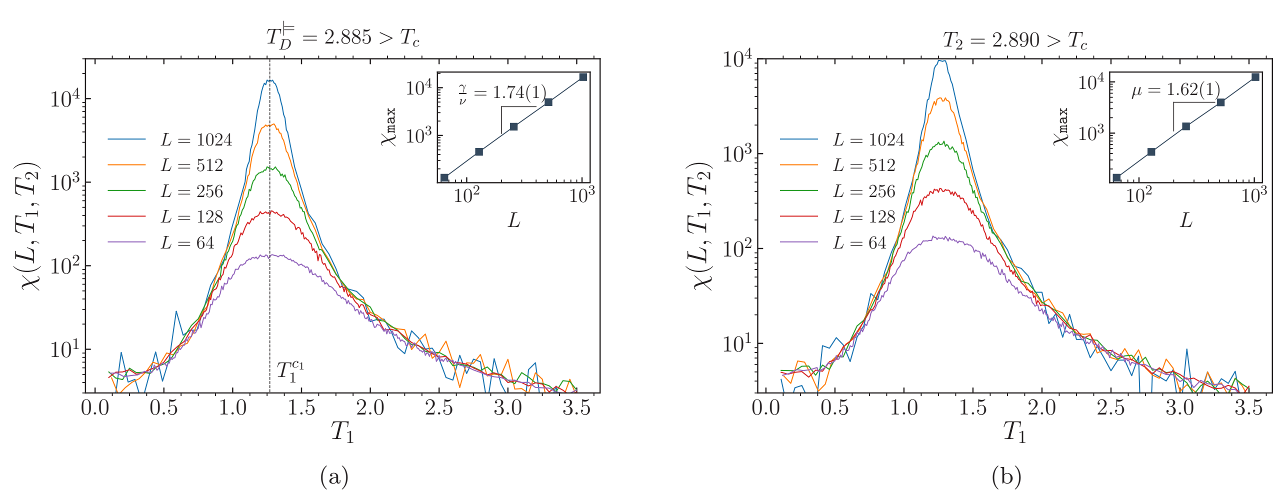


FIG. 9. (a) Magnetic susceptibility ($\chi$) for various system sizes in fixed $T_D^{\models} = 2.885 > T_c$. The inset: $\chi_{\max}$ in terms of system size in which $\gamma/\nu = 1.74 \pm 0.01$. (b) Magnetic susceptibility ($\chi$) for various system sizes in fixed $T_2 = 2.890 > T_D^{\models}$. The inset: $\chi_{\max}$ in terms of lattice size in $\mu = 1.62 \pm 0.01$.

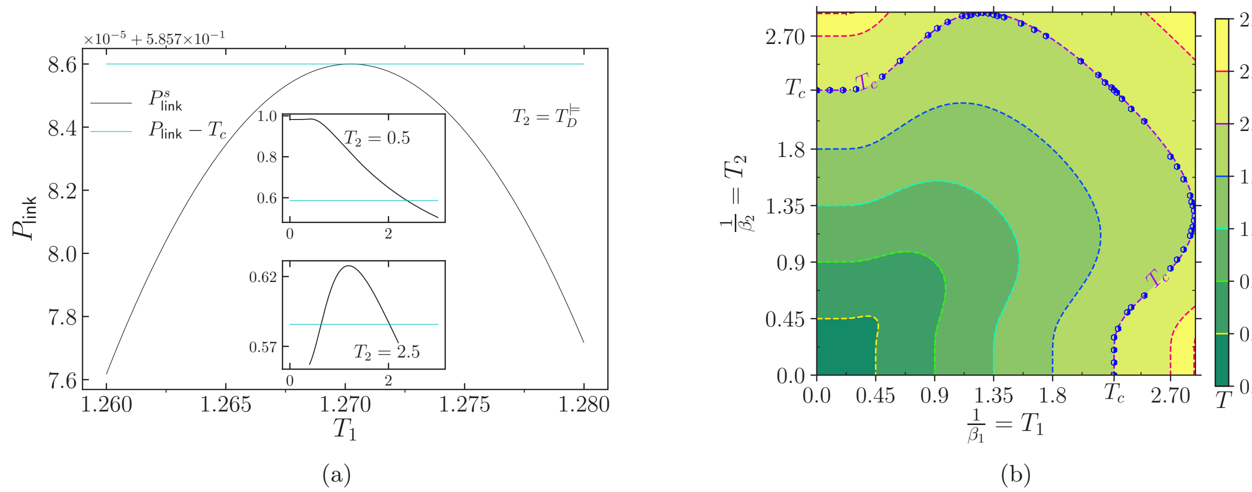

FIG. 10. (a) Probability of adding a spin to the evolving cluster ($P_{\rm link}$) in fixed in terms of $T_1$. The upper inset shows $P_{\rm link}$ in terms of $T_1$ for fixed $T_2 = 0.50$ and the bottom inset shows ($P_{\rm link}$) in terms of $T_1$ for fixed $T_2 = 2.50$. (b) Contour plot for Eq. (18) in $N = 0$. The dashed line represents $1/\beta = T$, and markers show critical points that we find in simulation.

we cannot map this system to a single-temperature system to capture all the physics of the system. The diluted cluster becomes self-similar (critical) at one single temperature for the single-temperature Ising model, and on a line for the two-temperature one. As we have seen, the model at the transition points is in the universality class of the Ising model, and the geometrical properties of the model does not change. Therefore, two objects (diluted clusters for the single- and the two-temperature Ising models) are almost the same due to the universality. Therefore, right at the criticality these two systems (at least, geometrically) become identical for which one can define an effective temperature in the single-temperature Ising model.

On this line, the corresponding FK cluster becomes critical (showing fractal properties [44,46]), undergoing a percolation transition, alongside with order-disorder transition. Our results above show that the effective system at the order-disorder transition points exhibits the same properties as the critical Ising universality class.

As a consistency check, we analyzed the crossing points of the left- and right-hand sides of Eq. (18) in Fig. 10(b) where it is shown that, for example, when one sets $T_2 = T_D^{\models}$ the curves cross each other at $T_1 = T_D^{\vdash}$ as expected. The insets show two other situations. In the upper inset of Fig. 10(b) for $T_2 = 0.50$ the crossing takes place in $T_1 = 2.376 = T_1^{c_1}$, just where we found the critical point, and for $T_2 = 2.50$ two crossing points are found. For all temperatures $T_2 > T_D^{\models}$ the two graphs never cross.

Before ending this section, it is worth noting that our paper is different from what has already been performed in the literature that we reviewed as the *first category*. In these papers the authors have concentrated mainly on the systems in which the temperature has a *spatial pattern*, meaning that the temperature (two values, chosen randomly in Ref. [14]) is distributed over the sample at a completely random manner or in a correlated pattern. For example, in Ref. [14] each site is kept in a different fixed single temperature which varies site to site so that the heat bath plays a key role. But in our model based on superstatistics concepts and the superposition of Boltzmann factors, each site of the system is in a fluctuating state between two temperatures for which the term “a hybrid state” or the “superposition of the Boltzmann factor” seems reasonable. In fact, the two temperatures are simultaneously applied to all sites over the system and all bands. We should state here that Ref. [14] concludes that the ferroparamagnetic transition in their model is in the Ising universality class. We should recall that all previous works have used the Ref. [14] method in which was used single temperature that varies site to site.

## IV. CONCLUSION

The previous studies on the two-temperature Ising model included local temperatures called heat baths. In these systems each site or part of the system with different probabilities stay in different heat baths. We redefine this concept and combine it with a superstatistic concept.

As an example of the SCP, we consider the Ising model with a distribution of temperature. This distribution was considered to be a binary one with two temperatures $T_1$ and $T_2$ as the simplest generalization. This two-temperature Ising model was numerically simulated on a square lattice with the Monte Carlo method. We developed Metropolis and SW algorithms for this system using the analogy with the one-temperature system and corresponding to the two-level Boltzmann factor. We numerically showed that the system undergoes an order-disorder transition which defines a critical line in $(T_1, T_2)$ phase space, see Fig. 3. The critical points were found using the data collapse analysis as well as the Binder’s cumulant method, which are consistent with the points that the heat capacity and the magnetic susceptibility show peaks. For all temperatures under $T_c^{\rm Ising}$ (the critical temperature of the ordinary Ising system) one second-order phase transition was observed, whereas for $T_c^{\rm Ising} < T_2 < T_D^{\models}$ two second-order phase transition, and for $T_2 > T_D^{\models}$ no transition takes place. Our numerical estimation of the critical exponents corresponding to the heat capacity and magnetic susceptibility, and the exponents of the order parameter (average magnetism) all illustrate that all points on the critical line belong to the ordinary Ising universality class.

To understand the structure of the critical line, we made an analogous effective system with a link probability $P_{\text{link}}(\beta_{\text{eff}})$ that is identical to the one for the binary temperature system, i.e., $P_{\text{link}}(\beta_1, \beta_2)$. Using this we obtained an analytical expression for the critical line, which matches perfectly with the numerical results, see Fig. 10(a). This study can be generalized to other more sophisticated distributions of temperature. This forms our ideas for further studying the superstatistic critical phenomena.

## APPENDIX: $n - \beta$ SUPERPOSITION

The Potts model is a generalization of the Ising model to more than two components ($q$ state). The Hamiltonian of this model in the zero magnetic field is defined as follows [41]:

$$H = -K \sum_{\langle i,j \rangle} \left( \delta_{\sigma_i \sigma_j} - 1 \right), \tag{A1}$$

where the spins take on the values of $1, 2, \ldots, q$, and $\delta$ is the Dirac $\delta$ function, and comparing the Ising and Potts Hamiltonians one can understand that $J = \frac{1}{2}K$.

This system in addition to the theoretical aspect that it investigate critical properties in order-disorder phase transition [47] is also possible to realize the Potts model in experiments [48]. The Potts model is related to a number of other outstanding problems in lattice statisticlike vertex model [49], percolation ($q = 1$ limit) [50], and resistor network ($q = 0$ limit) [51]. These are reasons to give motivation for investigating the Ising model in more general form and in combination with the Potts model with superstatistic concept. In the more general form of the Ising model in addition to the $q$ state (the $q$-spin component) we add the $n$-temperature component with the same probability and propose a $q$-state $n$-temperature Potts model.

Let us define the probability distribution of $\beta$ as follows:

$$f(\beta) = \frac{\delta(\beta - \beta_1) + \delta(\beta - \beta_2) + \cdots + \delta(\beta - \beta_n)}{n}. \tag{A2}$$

Using Eq. (1), a generalized $n$-level Boltzmann factor (nLBF) is obtained as follows:

$$B_n(E) = \frac{1}{n}(e^{-\beta_1 E} + e^{-\beta_2 E} + \cdots + e^{-\beta_n E}), \tag{A3}$$

the changes in total energy due to the single spin flip is changed to $E' = E + \delta E$. According to Eq. (8) for $p^{n\text{LBF}}(\beta_1, \beta_1, \ldots, \beta_n)$,

$$p^{n\text{LBF}}(\beta_1, \beta_1, \ldots, \beta_n) \equiv \frac{B_n(E')}{B_n(E)} = \frac{e^{-\beta_1 E'} + e^{-\beta_2 E'} + \cdots + e^{-\beta_n E'}}{e^{-\beta_1 E} + e^{-\beta_2 E} + \cdots + e^{-\beta_n E}}. \tag{A4}$$

We simplify the above equation,

$$p^{n\text{LBF}} = \frac{e^{-\beta_1 \delta E}}{1 + e^{-(\beta_2-\beta_1)E} + e^{-(\beta_3-\beta_1)E} + \cdots + e^{-(\beta_n-\beta_1)E}} + \frac{e^{-\beta_2 \delta E}}{1 + e^{-(\beta_1-\beta_2)E} + e^{-(\beta_3-\beta_2)E} + \cdots + e^{-(\beta_n-\beta_2)E}} + \cdots + \frac{e^{-\beta_n \delta E}}{1 + e^{-(\beta_2-\beta_n)E} + e^{-(\beta_3-\beta_n)E} + \cdots + e^{-(\beta_{n-1}-\beta_n)E}}. \tag{A5}$$

It can be written in a series form as follows:

$$p^{n\text{LBF}} = \sum_{i=1}^{n} \frac{e^{-\beta_i \delta E}}{\sum_{j=1}^{n} e^{-(\beta_j - \beta_i)E}}. \tag{A6}$$

At last, similar to Eq. (12) in the SW algorithm,

$$P_{\text{link}}^{n} = \sum_{i=1}^{n} \frac{1 - e^{-\beta_i}}{\sum_{j=1}^{n} e^{(\beta_j - \beta_i)}}. \tag{A7}$$


[1] C. Beck and E. Cohen, Physica A **322**, 267 (2003).
[2] C. Beck, Continuum Mech. Thermodyn. **16**, 293 (2004).
[3] C. Beck, Physica D **193**, 195 (2004).
[4] G. Wilk and Z. Włodarczyk, Phys. Rev. Lett. **84**, 2770 (2000).
[5] A. M. Reynolds, Phys. Rev. Lett. **91**, 084503 (2003).
[6] C. Beck, Phys. Rev. Lett. **98**, 064502 (2007).
[7] C. Beck, Phys. Rev. Lett. **87**, 180601 (2001).
[8] M. Baiesi, M. Paczuski, and A. L. Stella, Phys. Rev. Lett. **96**, 051103 (2006).
[9] I. Rouse and S. Willitsch, Phys. Rev. Lett. **118**, 143401 (2017).
[10] N. A. Alves and R. B. Frigori, Physica A **446**, 195 (2016)
[11] K. Ourbah and M. Tribeche, Phys. Lett. A **381**, 2659 (2017).
[12] K. Ourabah and M. Tribeche, Phys. Rev. E **95**, 042111 (2017).
[13] P. Garrido, A. Labarta, and J. Marro, J. Stat. Phys. **49**, 551 (1987).
[14] P. Tamayo, F. J. Alexander, and R. Gupta, Phys. Rev. E **50**, 3474 (1994).
[15] L. Li and M. Pleimling, Europhys. Lett. **98**, 30004 (2012).
[16] P. L. Garrido, J. Marro, and J. M. González-Miranda, Phys. Rev. A **40**, 5802 (1989).
[17] N. Borchers, M. Pleimling, and R. K. P. Zia, Phys. Rev. E **90**, 062113 (2014).
[18] H. Blote, J. Heringa, A. Hoogland, and R. Zia, J. Phys. A **23**, 3799 (1990).
[19] A. Szolnoki, Phys. Rev. E **60**, 2425 (1999).
[20] K. E. Bassler and Z. Rácz, Phys. Rev. Lett. **73**, 1320 (1994).
[21] B. Renklioglu and M. Yalabik, Eur. Phys. J. B **85**, 398 (2012).
[22] P. I. Hurtado, P. L. Garrido, and J. Marro, Phys. Rev. B **70**, 245409 (2004).
[23] C. Beck, Braz. J. Phys. **39**, 357 (2009).
[24] A. Iliopoulos, D. Chorozoglou, C. Kourouklas, O. Mangira, and E. Papadimitriou, Bollettino di Geofisica Teorica ed Applicata **60**, 531 (2019).
[25] K. Briggs and C. Beck, Physica A **378**, 498 (2007).

[26] B. M. McCoy and T. T. Wu, *The Two-Dimensional Ising Model* (Courier, Mineola, NY, 2014).
[27] C.-K. Hu, Phys. Rev. B **29**, 5103 (1984).
[28] M. N. Najafi, J. Cheraghalizadeh, and H. J. Herrmann, Phys. Rev. E **100**, 042132 (2019).
[29] M. Najafi, J. Stat. Mech.: Theory Exp. (2015) P05009.
[30] M. M. Tsypin and H. W. J. Blöte, Phys. Rev. E **62**, 73 (2000).
[31] G. Mussardo, *Statistical Field Theory: An Introduction to Exactly Solved Models in Statistical Physics* (Oxford University Press, Oxford, 2010).
[32] P. Francesco, P. Mathieu, and D. Sénéchal, *Conformal Field Theory* (Springer, Berlin, 2012).
[33] P. Bak, C. Tang, and K. Wiesenfeld, Phys. Rev. Lett. **59**, 381 (1987).
[34] P. Bak, C. Tang, and K. Wiesenfeld, Phys. Rev. A **38**, 364 (1988).
[35] M. N. Najafi, J. Cheraghalizadeh, M. Luković, and H. J. Herrmann, Phys. Rev. E **101**, 032116 (2020).
[36] J. Cheraghalizadeh, M. N. Najafi, H. Dashti-Naserabadi, and H. Mohammadzadeh, Phys. Rev. E **96**, 052127 (2017).
[37] M. Najafi, J. Phys. A: Math. Theor. **51**, 175001 (2018).
[38] M. Najafi, M. Ghaedi, and S. Moghimi-Araghi, Physica A **445**, 102 (2016).
[39] J. Cheraghalizadeh and M. Najafi, Phys. Scr. **94**, 095204 (2019).
[40] J. Cheraghalizadeh, M. N. Najafi, H. Mohammadzadeh, and A. Saber, Phys. Rev. E **97**, 042128 (2018).
[41] R. H. Swendsen and J.-S. Wang, Phys. Rev. Lett. **58**, 86 (1987).
[42] F. Sattin, Phys. Lett. A **382**, 2551 (2018).
[43] R. Hanel, S. Thurner, and M. Gell-Mann, Proc. Natl. Acad. Sci. U.S.A. **108**, 6390 (2011).
[44] W. Janke and A. M. Schakel, Nucl. Phys. B **700**, 385 (2004).
[45] W. Selke, Eur. Phys. J. B **51**, 223 (2006).
[46] R. Vasseur and J. L. Jacobsen, J. Phys. A: Math. Theor. **45**, 165001 (2012).
[47] F.-Y. Wu, Rev. Mod. Phys. **54**, 235 (1982).
[48] E. Domany, M. Schick, J. S. Walker, and R. B. Griffiths, Phys. Rev. B **18**, 2209 (1978).
[49] H. N. Temperley and E. H. Lieb, Proc. R. Soc. London, Ser. A **322**, 251 (1971).
[50] J. W. Essam, Rep. Prog. Phys. **43**, 833 (1980).
[51] C. M. Fortuin and P. W. Kasteleyn, Physica **57**, 536 (1972).